

The special capabilities of Surface Constructor kinematic modelling and simulation software

L Dudás

Department of Information Engineering, University of Miskolc, Miskolc, Hungary
E-mail: iitdl@uni-miskolc.hu

Abstract. The paper introduces the innovative and unique capabilities of the Surface Constructor software application. This tool is intended for modelling and optimizing mating enveloping surfaces that can be used e.g. as tooth surface of gears. The software applies the original Reaching Model theory that can provide surface enveloped by a given surface. The theory handles local and global methods, generating not only the enveloped surface but all the types of local undercuts and global cut such a way. Surfaces and kinematic relations are represented by symbolic algebraic expressions giving the maximal freedom in modelling. Special capability of the tool is showing the $R = R(\Phi)$ functions that can explore and qualify the abnormalities in mating of surfaces. Moreover it provides special velocity-space features that can reveal the nature and characteristics of the space where motions happen. The tool can apply intermediary generating surface making also possible generating mating surfaces characterized by point-like contact. All these unique features integrated in a complex design system that uses symbolic, numerical and visual representations of the modelled objects. The paper demonstrates every capability of the software tool with concrete applications, in some cases with patented solutions.

1. Introduction

The paper gives an overall overview and demonstration of the capabilities of the *Surface Constructor* (SC) enveloped surface generator and kinematical modelling software application. In the last decades this software got name as a versatile and powerful tool proving its capabilities in solving different innovation tasks. Its success origins from the fact that one of the requirements of the machine industry is to resolve the general task of conjugate surface pairs, so generate surface by other moving surface and this task is not solvable easily by usual 3D CAD applications. The most important area is designing and machining gearings and their tools. For the resolving such tasks the SC includes a novel enveloped surface determination theory, the *Reaching Model*. This theory solves the general task of meshing surfaces fully including the detection of all the possible types of undercut situations. This fundamental theory underlies the SC tool and will be detailed in the second section.

SC works similarly to the well-known 3D CAD applications, gives a universal and task type independent environment for modelling enveloping surfaces and analysing their mesh properties and animating their motion. The three-level structure of the application that provides this flexibility and versatility will be described shortly in the third section.

Then, in the fourth section the unique capabilities will be introduced and demonstrated through example tasks. The first speciality will describe the visualization and use of the $R = R(\Phi)$ functions. The second speciality will be the visualization of the velocity-space properties, while the capability of



using intermediary theoretical surface and creating such a way surface pairs that mate point-like manner will be demonstrated as the third special feature.

2. The core theory: the *Reaching Model*

There are two well-known existing methods to determine the enveloped surface [1]:

- the differential-geometric method developed by *Gochman*, and
- the kinematical method, which applies the $\mathbf{n} \cdot \mathbf{v}^{1,2} = 0$ product where \mathbf{n} is the normal vector and $\mathbf{v}^{1,2}$ is the relative velocity at the meshing point.

These quick analytical methods are local methods, so they can work in infinitely small space and time domain and they can produce the local undercuts or the boundary of required enveloped surface. As a consequence, these methods are suitable for detecting all types of local undercuts, which can appear in an infinite small domain but fail in determination of the real surface if it has swept region which accompanies to local undercut almost every time. The determination of such not enveloped part of surfaces need global surface determination method, like the more slow discrete digital simulation of the surface generation.

In the last decades researchers have been applied computers for enveloped surface modelling expansively. Among the pioneers *Holler* produced worm-gear and hypoid-gear surfaces using computer model of meshing and local method [2]. Later *Weck* and his colleague applied computer simulation of cutting process and global method to produce different types of gears [3].

Other researchers used both local and global methods to determine quantity of the interference. *Seveleva* computed a *Gleason* bevel gear tooth surface using theory of enveloping surfaces and numerical simulation of cutting at the same time [4]. In our days the most famous gear investigator in addition to the others, who uses discrete digital simulation is *Lunin* in its gear development institute *ZAKGEAR* [5].

It is necessary to emphasize that the above-mentioned researchers and their papers did not use the local-global terminology. The original model of the author proposed in the next section gives a consistent and easy to understand resolution of enveloping surfaces and all the types of local undercuts and global cut. This theory, that gives the core of the algorithm of *SC* software application, proved its fullness, power and versatility in solving many concrete tasks.

2.1. The general task

Given the generating surface $F1$ in coordinate system $K1$ by vector $\mathbf{r1} = \mathbf{r1}(x1, y1, z1)$ as shown in figure 1, and given the relative motion between $K1$ and $K2$ coordinate systems. Surface $F2$ has to be generated by surface $F1$ in the coordinate system $K2$ as vector $\mathbf{r2} = \mathbf{r2}(x2, y2, z2)$. The figure shows a general contacting point P and its trajectory d in the $K1$ coordinate system.

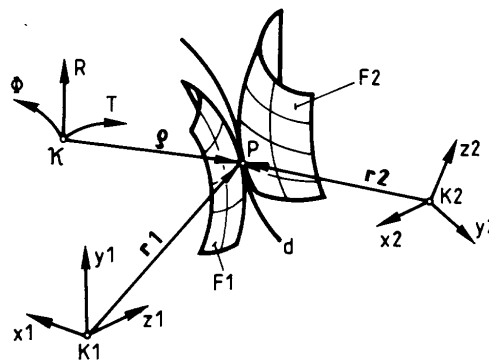


Figure 1. The applied coordinate systems in generation $F2$ by $F1$.

The *Reaching Model* applies a special non-Descartes coordinate system κ . The Φ coordinate lines as well as the coordinate axis Φ itself coincide with the trajectory of the moving points of a surface that is in the coordinate system $K2$ so Φ has two roles: 1. motion (time) parameter, 2. one of the three space coordinates of coordinate system κ . When the motion of $K2$ starts this surface coincides with the R – T coordinate surface of coordinate system κ . The vector $\rho = \rho(\Phi, R, T)$ gives the generating surface $F1$ in the coordinate system κ with its general point P . The R and T coordinate directions are set up using suitable shape and relation to Φ coordinate lines. The $K1$ and κ coordinate systems are fixed to each other.

2.2. The reaching process to generate one point of the generated surface $F2$

The reaching process is demonstrated in figure 2.a. In the reaching process we choose a Φ coordinate line that does not intersect $T1$. Stepping from one Φ coordinate line to another going R direction, the generating Φ coordinate line will be that, which can reach $F1$ first. This Φ line is the trajectory of point P_k' that will be one surface point of generated surface $F2$. Point P_k will be the meshing point. Using the κ_i coordinate system we can determine one curve of the generated surface $F2$ like a set of points. Applying a series of different κ coordinate systems from κ_0 to κ_s using a new Z parameter the full generated surface $F2$ can be got as a series of curves. Looking at figure 2.b it can be recognized that to find the contacting point P_k using the reaching process is equal to resolve a minimum-value problem. This easy task becomes evident if the curved Φ – R surface has been transformed into a plane with straight Φ – R coordinate axes. Due to the aforementioned the complex task of determining surface $F2$ and recognizing all the types of local undercuts can be replaced with resolution and discussion of a minimum-value problem. Detailed description and examples of local undercuts and global cuts are given in [6].

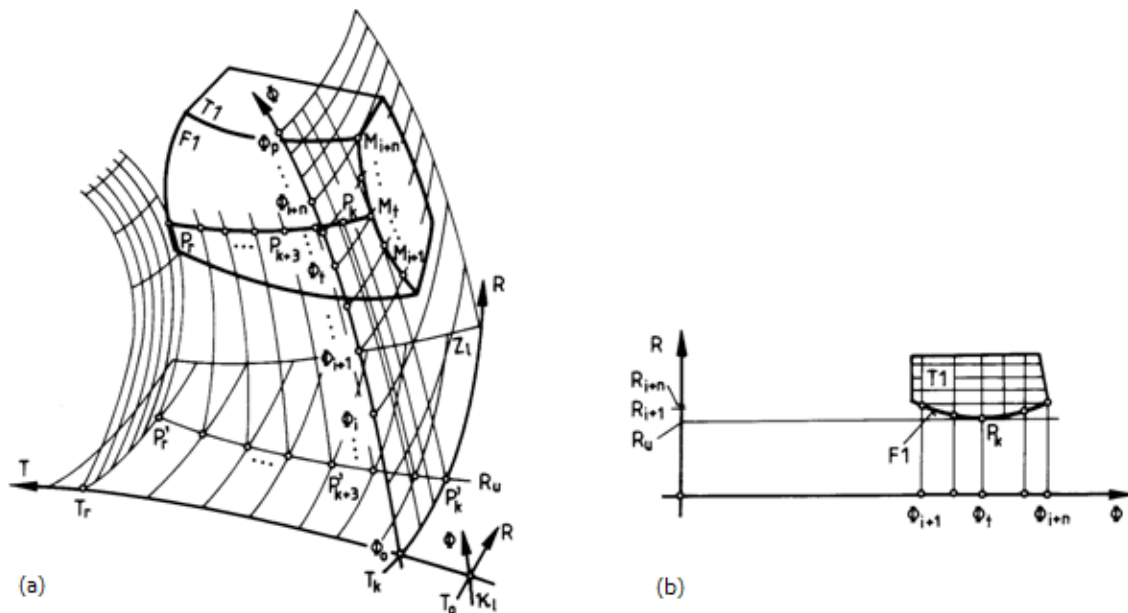


Figure 2. Determining one meshing point of $F2$ is equivalent to solve a minimum value task.

3. The Surface Constructor software

The *Surface Constructor* computer program implements the theory. The structure of a newer improved version is shown in figure 3. This version can utilize more generating surfaces one after another and can also produce point-like contact between more generated surface pairs. The software has three levels:

- Symbolic representation of input objects
- Numerical representation of input and computed objects
- Visualization and simulation possibilities.

Among the unique capabilities there is the inbuilt symbolic algebraic computation [7] for manipulation of input expressions and for multiplying the automatically created symbolic transformation matrices, see figure 4. The *SC* program is able to demonstrate the motion of the elements in maximum eleven independent opened visualization windows and can visualize the different features of the analysed kinematical problem e.g. wandering of meshing line dynamically. The selection and visualization options are as follows:

- *F2glob*: global computational method and the surface calculated with it
- *F2lok*: local computational method and the resulted surface points and meshing lines
- *F2al*: computation and visualization of the variations of local undercuts
- Φ : computation and visualization of trajectories of selected points
- $R-\Phi$: computation and visualization of $R = R(\Phi)$ functions as a special feature of this software
- v_a : computation and visualization of the space of relative velocity and acceleration
- PT : computation and visualization of axoids and features of velocity screw.

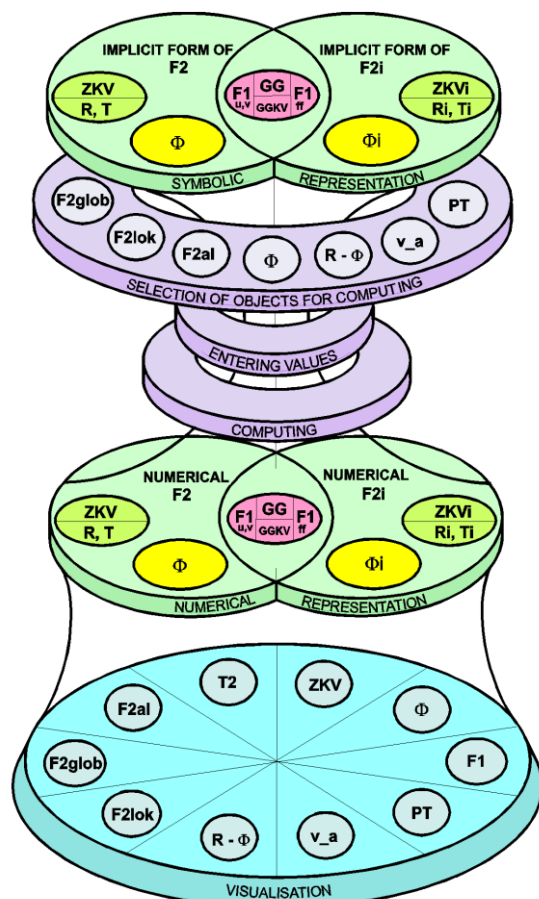


Figure 3. The symbolic, the numerical and the visual representation levels in *SC*. Before calculations and for visualization different objects can be preselected.

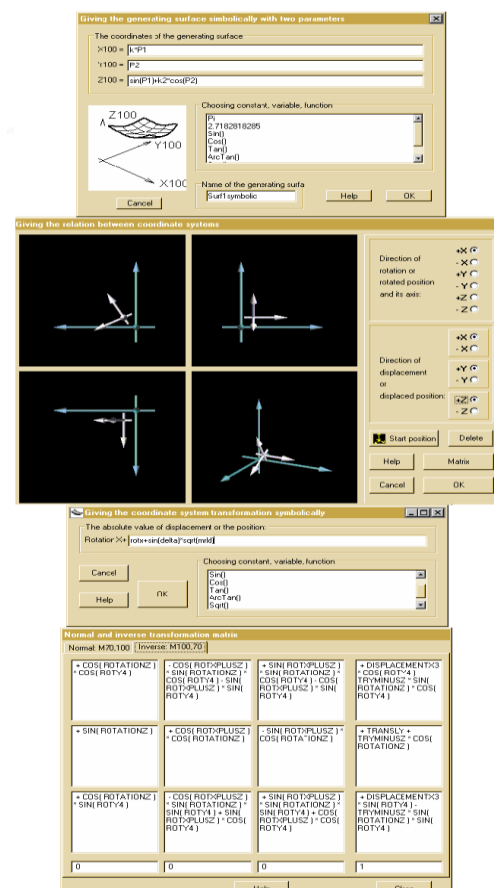


Figure 4. Curves and surfaces can be entered with symbolic expressions, symbolic transformation matrices are generated automatically.

In case of analysis of point-like mesh the generated members of a gearing are surfaces $F2i$, e.g. $F2_1$ and $F2_2$. The intermediary theoretical generating surface between them is $F1$. $F1$ can be give with GG generating curve as a swept surface or as a two-parametric surface $F1 = F1(u,v)$. The third planned variant is giving $F1$ as free form (ff) surface with spline. The kinematic relations that define the generating motions are given by automatically created symbolic transformation matrices as functions of Φi , e.g. $\Phi 1$ and $\Phi 2$ motion parameters. The $ZKVi$ kinematic relations and the Ri and Ti parameters are used in the algorithm realising the *Reaching Model*.

4. Introducing some of the additional unique capabilities

These capabilities will be presented through examples. First the $R = R(\Phi)$ functions will be introduced that can explore and qualify the abnormalities of the generated surface. Then the special velocity-space features of the velocity screw will be demonstrated that can reveal the nature and characteristics of the space where motions happen. Finally the possible use of intermediary generating surface will be exemplified making possible generating mating surfaces with point-like contact.

4.1. Visualization of $R = R(\Phi)$ functions

The power of $R = R(\Phi)$ functions comes from the main role of them in *Reaching Theory*. As figure 2(b) shows the minimum point of this function generates a meshing point in the enveloping that corresponds to one of the generated point of the $F2$ generated surface. To exploit this power SC includes a special window that mappings the $P_k = [T_k; Z_l]$ points of the generated $F2$ surface into the points of this window. Figure 5 shows a surface generation by a parabolic surface (a) and the corresponding $R = R(\Phi)$ functions visualizing window that corresponds to the $F2 = F2(T,K)$ parametric representation (b). The window can visualize the $R = R(\Phi)$ function for every point of $F2$ as a small function curve as shown in figure 5(b).

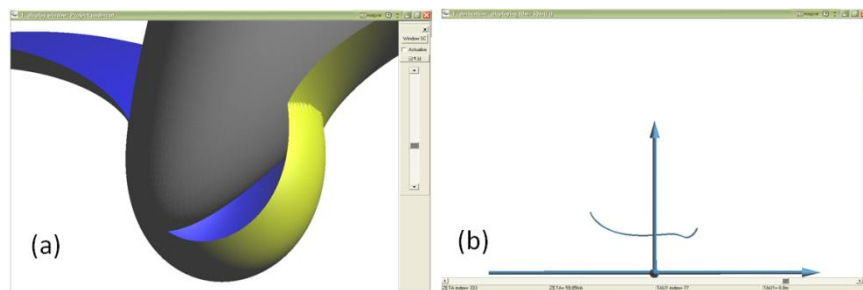


Figure 5. Global cut type interference on the generated surface (a) and detecting it as special shape of the $R = R(\Phi)$ function (b).

Moving the mouse cursor in the window, the $R = R(\Phi)$ function curve that corresponds to the $[T,K]$ parameters of $F2$ appears instantly. Moving the mouse cursor in the window the $R = R(\Phi)$ function for any point of $F2$ can be visualized. This is a comfortable way for analysing these function curves. As the shape of this function curves can reveal the undercut situations, this visualization capability of SC can be used advantageously. The local *minimum* point means healthy generated point of $F2$. A *maximum* point means a generated point which is a local undercut point because its neighbour points are globally cut points. The typical form of the local undercut is an *inflexion* shape having horizontal tangent on the $R = R(\Phi)$ function curve.

The concrete example shown in figure 5 introduces both local undercut and global cut. As the undercut that can be determined by local mathematical methods is a point-like phenomenon and in this example – and usually – the motion is not limited to a point, the continued motion causes global cut that removes the previously enveloped surface region, such way decreasing the area of the connecting surface. Figure 5a shows when the parabolic generating body destroys the previously enveloped part of the lower surface in the continued motion causing global cut and resulting in an edge on the surface.

The right window shows this situation with the corresponding $R = R(\Phi)$ function curve where R is the vertical reaching direction and Φ is the motion parameter measured along the horizontal axis. The left minimum point of the curve results in an enveloped point that will be destroyed later by the right lower minimum point, which is the generator point of one of the points of the enveloped undercut surface. The detailed explanation of the *Reaching Model* with detailed explanation of undercut phenomenon can be found in [8].

The $R = R(\Phi)$ function curves visualization window has a more comfortable visualization possibility for detecting undercuts. In this possibility all the function curves having the same value of Z or $T F2$ surface parameter can be shown as a surface. In this method changing the other parameter the full surface of $F2$ can be checked against undercut through the set of appearing checking surfaces. The demonstrative example solves the next task: given a special quasi-helical surface as a compressor rotor characterised by changing pitch. The grinding of such special helicoids needs a special grinding machine invented by the author [9]. The grinding wheel of this machine has a working surface created enveloping the grinding wheel with the compressor rotor. Because the generated wheel surface is fairly complex, the checking against undercut is necessary. Figure 6 demonstrates the use of the mentioned checking method in case of this grinding wheel surface.

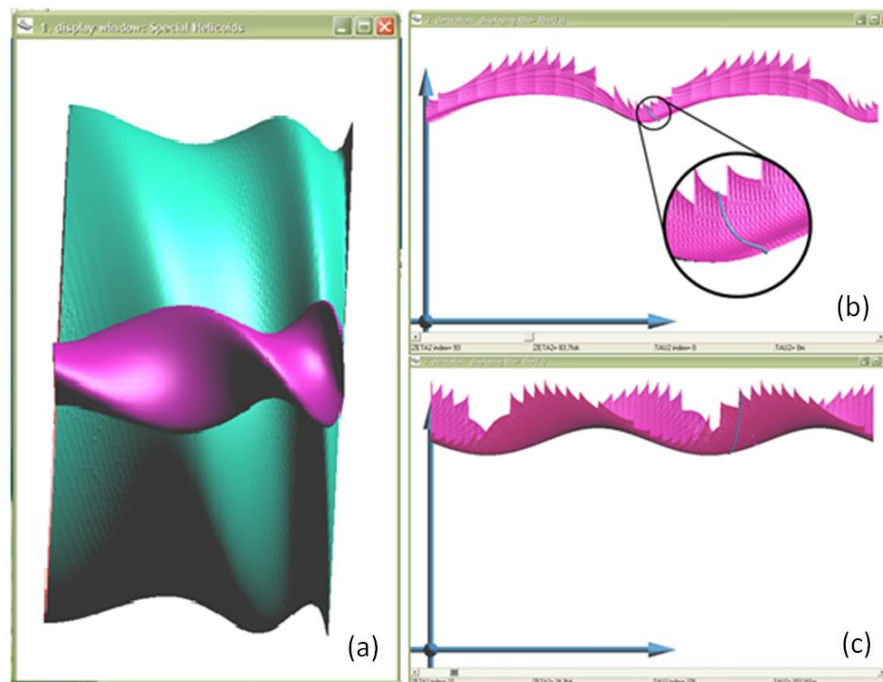


Figure 6. The rotor and the special grinding wheel (a), inflexion means undercut (b) and the perfect valley form of checking surface (c).

4.2. Velocity space features

One of the unique capabilities of SC is handling the velocity screw of the moment of the motion. The trajectories, the velocity vectors and the acceleration vectors can be visualized. The axis of the screw can be determined by SC and the set of axes can be displayed parallel to the motion. So the well known theoretical formation, the axoid of the motion can be visualized and analysed dynamic manner. Figure 7 expounds the velocity screw while figure 8 shows an example on moving point trajectories, on the axoid of the motion and on velocity and acceleration vectors of the motion along the trajectories.

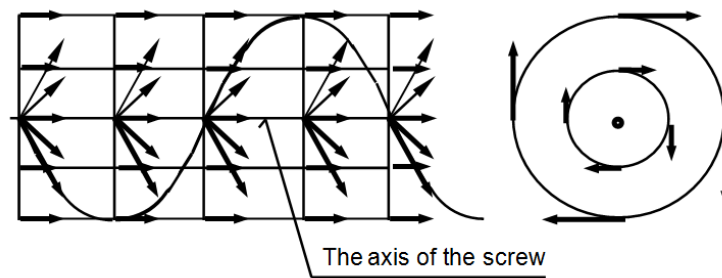


Figure 7. The velocity screw formed by the tangential to helical lines velocity vectors in a moment of the motion. Shown in two views.

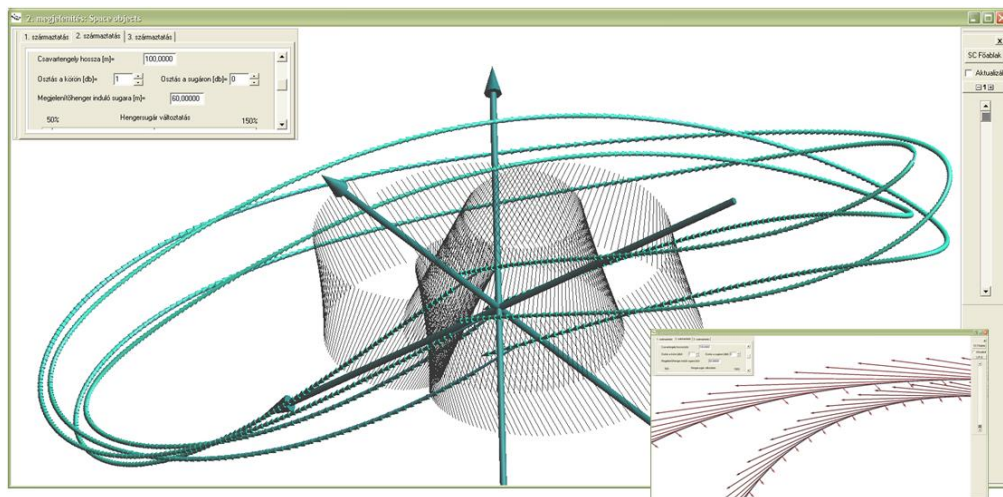


Figure 8. Trajectories of selected moving points and the set of velocity screw axes as an axoid. The small window shows velocity vectors that are tangential to the trajectories and acceleration vectors of the moving points.

Higher level space objects of the velocity space will be discussed in the next subsections. The base of the calculation was the determination of the axis of the velocity screw. It is known, that the spatial instantaneous motion of a rigid body can be represented by a velocity screw [10]. The calculation details are given in [6].

4.2.1. Visualizing the Velocity Screw. The goal of the visualization of the instantaneous velocity screw is to provide an imagination on the structure of the velocity space and to discover special moments when the space changes to simple rotation or translation momentarily, or the motion stops for a moment. The axis of the screw is a special loci itself where the points characterized by simple translation or standing, in case of instantaneous rotation. The space of velocity is demonstrated by spirals that give the direction of the tangential velocity vectors. The visualization mode gives the maximal freedom to analyze the space: scrolling the time-parameter scroll bar the motion can be animated with the continuously changing spirals. SC needs symbolic input of motions. After entering the numerical values the selection of the world coordinate system and the turning on the velocity space visualization follows. Eleven display windows can be used in the same time with different kinematical and visualization parameters providing maximum freedom in visual analysis. Here only some example window is given to make the possibilities felt. Figure 9(a) shows an axoid having elliptical form and the momentary screw.

4.2.2. Visualizing the Normal Set. The null-system is pictured by one normal set. The radius, the density and the position along one outer spiral can be modified. See figure 9(b). The set of normal sets forms the normal-complex of the screw. The cardinality of the normals in the normal-complex is ∞^3 .

4.2.3. Visualizing the Reciprocal Polars. Giving a line in the null-complex that is not a normal in the screw determines a second non-normal line. These lines determine each other unambiguously and play central role in the geometry of connection because they are the holder of a ∞^2 cardinality of normals in the normal-complex. See the reciprocal polars in figure 9(c).

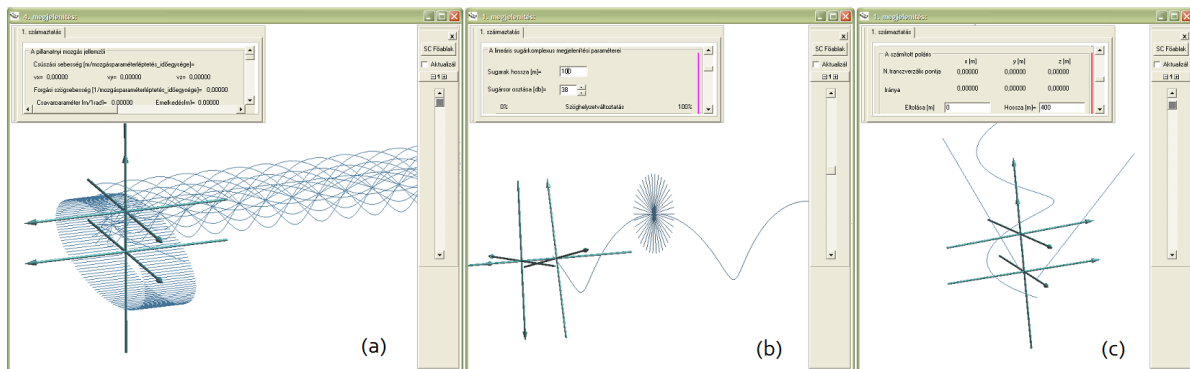


Figure 9. Elliptical axoid of the motion and the momentary screw (a), normal set (b) and reciprocal polars (c).

4.2.4. Visualizing the Linear Congruent. The set of normals that intersect the reciprocal polars forms the linear congruent. It is a ∞^2 cardinality formation of normals in the normal-complex. For the visualization of the congruent there are two ways. The first method can draw one or two normal sets on one or on two linear polars. The parameters of the figure of the normal set can be changed freely and the location on the linear polar can be modified by slider or entering the value manually. See figure 10(a). The second method draws all normals of the normal-complex that intersects the reciprocal polars in given number points. The density of this formation can be modified by up-down controls. Normal sets can be turned on and off additionally. See figure 10(b).

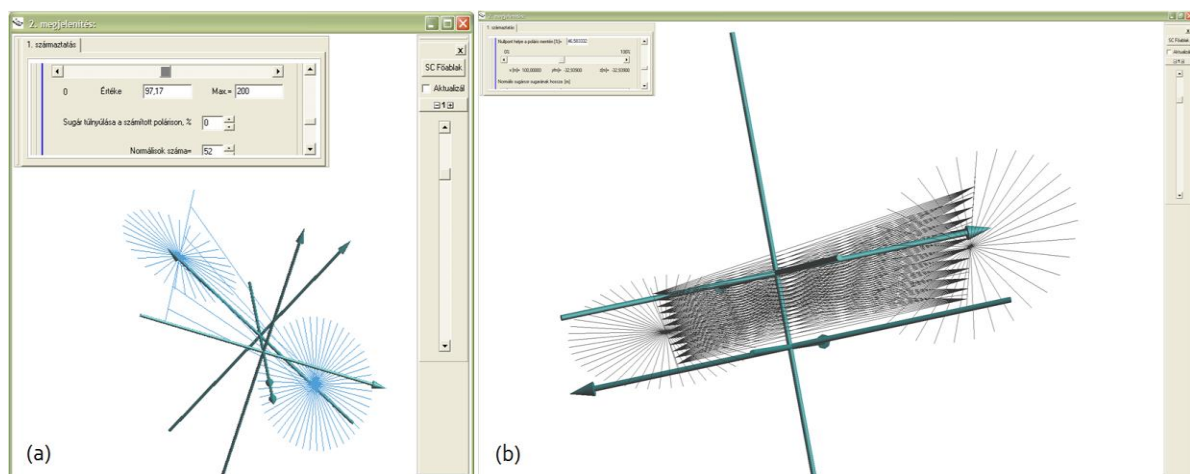


Figure 10. Normal sets on the reciprocal polars (a) and the linear congruent and two normal sets on the reciprocal polars (b).

4.3. Modeling point-like contact with intermediary generating surface

This capability simply repeats the enveloping process with the same generating $F1$ surface with different relative kinematics. See figure 11. The $F1$ generating surface is a swept by the $VG(p1)$ generating curve with $p2$ as the parameter of the sweeping motion. Using $F1$ as a common theoretical generating surface the $F2_1$ and $F2_2$ generated surfaces can be calculated. In the enveloping process of $F2_1$ the Φ_1 motion parameter determines the working of the generating kinematic between $K1$ and $K2_1$ coordinate systems while in the enveloping of $F2_2$ the Φ_2 plays a similar role activating the motion between $K1$ and $K2_2$ coordinate systems. The two generating processes result in conjugate to $F1$ generated surfaces that mesh with $F1$ in lines. Removing the theoretical $F1$ surface out of the two generated surfaces, the intersection point of the two momentarily meshing curves will remain as the contact point of $F2_1$ and $F2_2$. Such gearings having point-like contact are famous for good machining error and assembling error toleration and work with less noise and vibration.

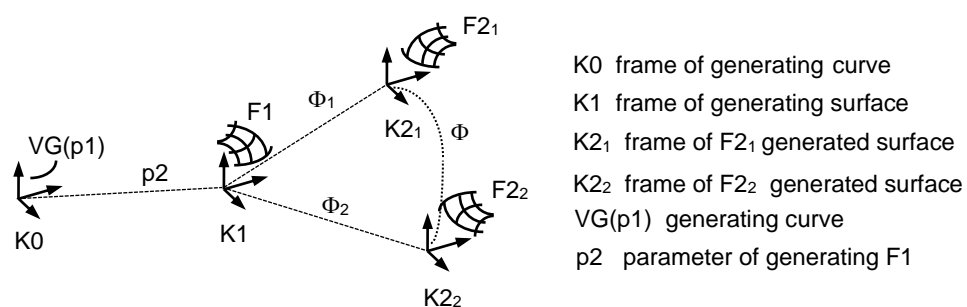


Figure 11. Meshing pair generation with intermediary generating surface $F1$.

The improvement of worm gearings and avoiding noise that can originate from backlash [11] and from not constant transfer ratio is important [5, 12]. The application example solves the problem of modified worm gearings [13, 14]. The profile or tooth modification applied to achieve noiseless and misalignment-tolerant worm gearings results in error in transmission generally. The use of intermediary generating surface for generation of worm gearing members solves this problem because produces transmission error free continuous point-like contact between the worm and the worm gear. Figure 12 demonstrates the working of the mentioned method in case of cylindrical worm gearing. Subfigure (a) shows the worm, the segment of the worm gear, the intermediary generating helicoids segment and the contact arc between the worm gear and the generating helicoid. Subfigure (b) shows three moments of the contact patch wandering. The dark patch on the arc is the momentary point-like contact pattern. The method is given in detailed form in [8].

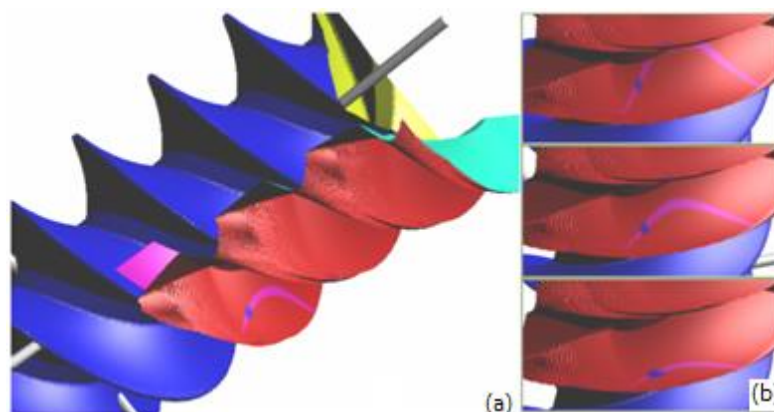


Figure 12. Visualization of worm gear surfaces having point-like meshing (a) and the animation of the contact patch wandering (b).

5. Summary

The paper focused on the unique capabilities of the SC software application. The modelling flexibility and fullness originate from the *Reaching Model* as the core theory and from the symbolic algebraic representation ability of the software realisation. A short description refreshed the structure and working of the software. In the main part of the paper, some solved task emphasised the unique capabilities of SC. The visualization of $R = R(\Phi)$ functions help detecting and avoiding local undercuts and global cut. The peerless spatial velocity space object visualisation capability helps to reveal the best regions of the velocity space for optimization of gearings. Then the method of producing cylindrical worm gearings having point-like connection was demonstrated. The advantage of this master technique is that the point-like connection was realised without the ruining of the exact motion transfer that was made by the previously published suggestions. These examples prove the applicability of SC for gear investigation and innovation. Figure 13 demonstrates the profuseness and the ease of use of this tool in enveloped surfaces development and improvement.

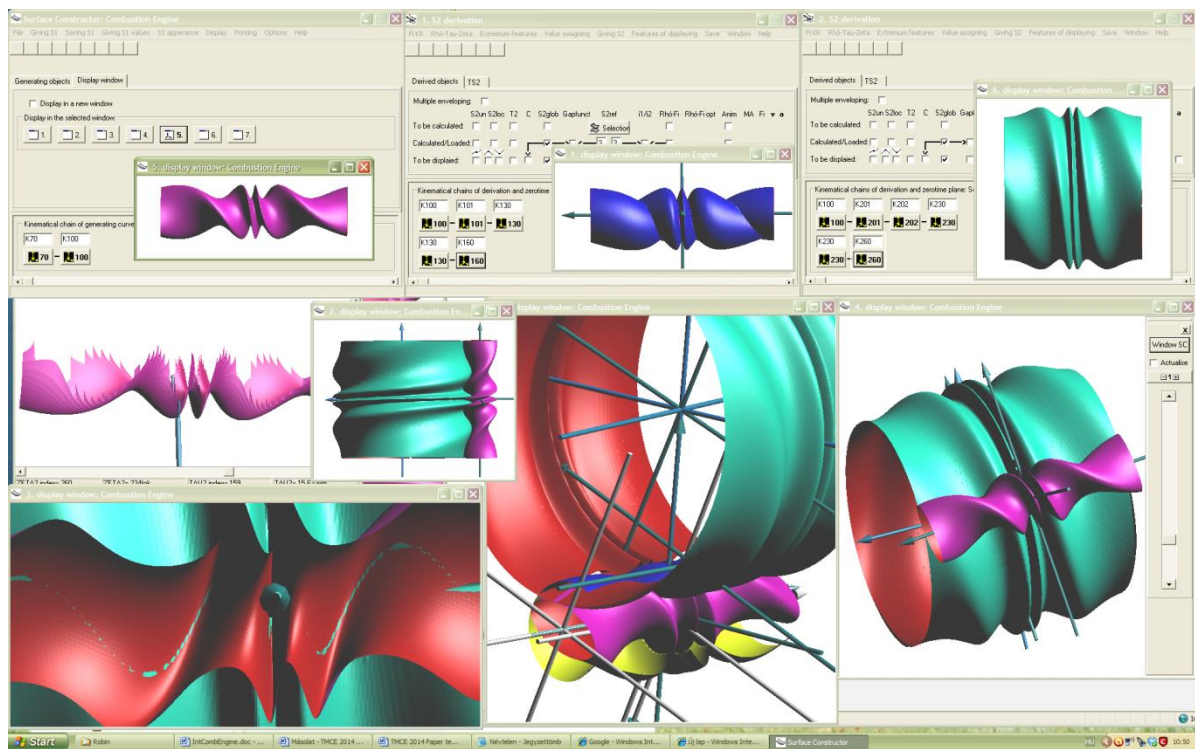


Figure 13. Designing the rotor, the rotary chamber and the grinding wheel surface for a patented rotary internal combustion engine [15].

Acknowledgments

This research was partially carried out in the framework of the Center of Excellence of Mechatronics and Logistics at the University of Miskolc. The described study additionally was carried out as part of the EFOP-3.6.1-16-00011 “Younger and Renewing University – Innovative Knowledge City – institutional development of the University of Miskolc aiming at intelligent specialization” project implemented in the framework of the Széchenyi 2020 program. The realization of this project is supported by the European Union, co-financed by the European Social Fund. The financial support is acknowledged.

References

- [1] Litvin F L 1994 *Gear Geometry and Applied Theory* Prentice Hall, Englewood Cliffs, NJ.

- [2] Holler R 1976 *Rechnersimulation der Kinematik und 3D-Messung der Flankengeometrie von Schneckengetrieben und Kegelradern*, PhD Thesis, TH Aachen
- [3] Weck M and Reuter W 1989 Optimiertes Verzahnungs-scleifen durch rechnergestützte Verfahrenssimulation *Industrie-Anzeiger* **95** 28–31.
- [4] Seveleva G I, Gundaev S A and Pogorelov V S 1989 Numerical modelling of cutting tapered gears having teeth with circular arc form (in Russian) *Vectnik Masinoctroenia* **3** 44–7
- [5] Lunin S 2009 *Design of Worm Gears for Low Noise Applications Using Worm Gear Software from ZAKGEAR*, <http://www.zakgear.com/Worm.html>, Accessed: 05.20.2018.
- [6] Dudás L 2010 New way for the innovation of gear types *Engineering the Future* ed. L Dudás (InTech) pp 111–40
- [7] Lazard D 1979 Systems of algebraic equations *Symbolic and Algebraic Computation, Lecture Notes in Computer Science* Eurosam '79, An International Symposium on Symbolic and Algebraic Manipulation, Marseille, France, ed E W Ng, pp 88–94
- [8] Dudás L 2010 Modelling and simulation of a novel worm gear drive having point-like contact, *Proceedings of TMCE 2010 Symposium*, Horváth, I.; Mandorli, F. & Rusák, Z. (Ed.), pp. 685–98, ISBN 978-90-5155-060-3, Ancona, Italy, April 2010.
- [9] Dudás L 1992 *Grinding machine, for grinding non-surface of revolution surfaces, especially conical and globoid worms*, Hungarian patent HU P9003803
- [10] Xiao D Z and Yang A T 1989 Kinematics of three dimensional gearing, *Mech. Mach. Theory* **24** 245–55
- [11] Kacalak W, Majewski M and Budniak, Z 2016 Worm gear drives with adjustable backlash. *Journal of Mechanisms and Robotics* 8/014504-1
- [12] Bercsey T and Horák P 1999 Error analysis of worm gear pairs *Proc. 4th World Congress on Gearing and Power Transmissions. CNIT-PARIS France* 419–24
- [13] Ohshima F and Yoshino H, 2001 Ideal Tooth Surface Modification Method For Cylindrical Worm Gears *Proc. JSME International Conference on Motion and Power Transmissions VT:MPT I I(01-202)*, pp 460–5.
- [14] Seol I and Chung S 2000 Design and Simulation of Meshing of New Type of Worm-Gear Drive with Localized Contacts *KSME International Journal* **14** 408–17.
- [15] Dudás L 2017 Developing a rotary internal combustion engine characterised by high speed operation *Vehicle and Automotive Engineering. Lecture Notes in Mechanical Engineering*, ed K Jármay, B Bolló (Springer) pp 79–89